Korea-Australia Rheology Journal
Vol. 19, No. 1, March 2007 pp. 17-25

Transverse permeability measurement of a circular braided preform in liquid composite molding

Hee Sook Chae, Young Seok Song and Jae Ryoun Youn*
School of Materials Science and Engineering, Seoul National University, Seoul 151-742, Korea
(Received November 3, 2006; final revision received February 6, 2007)

Abstract

In liquid composite molding (LCM), composites are produced by impregnation of a dry preform with liquid resin. The resin flow through the preform is usually described by Darcy's law and the permeability tensor must be obtained for filling analysis. While the resin flow in the thickness direction can be neglected for thin parts, the resin flow in the transverse direction is important for thicker parts. However, the transverse permeability of the preform has not been investigated frequently. In this study, the transverse permeability was measured experimentally for five different fiber preforms. In order to verify the experimental results, the measured transverse permeability was compared with numerical results. Five different fiber mats were used in this study: glass fiber woven fabric, aramid fiber woven fabric, glass fiber random mat, glass fiber braided preform, and glass/aramid hybrid braided preform. The anisotropic braided preforms were manufactured by using a three dimensional braiding machine. The pressure was measured at the inlet and outlet positions with pressure transducers.

Keywords : glass fiber, aramid fiber, liquid composite molding, permeability, braiding

1. Introduction

In liquid composite molding (LCM), composite parts are produced by impregnation of the dry reinforcement with liquid matrix resin (Advani *et al.*, 1994; Jones, 1975). Permeability of the fiber assembly has been of special interest because determination of the permeability tensor for a fiber preform is essential for the flow analysis of LCM (Endruweit *et al.*, 2002; Wu *et al.*, 1994; Bechtold and Ye, 2003; Sadiq *et al.*, 1995; Sayre and Loos, 2003; Drapier *et al.*, 2002; Kim and Daniel, 2003; Weitzenböck *et al.*, 1998; Markicevic and Papathanasiou, 2003; Lim and Lee, 2000; Phelan Jr. and Wise, 1996). For thin parts, the resin flow in the thickness direction can be neglected and thin parts are considered as two-dimensional composites. Many investigations have been reported on determination of the in-plane permeability of fiber preforms (Gebart and Lidström, 1996; Amico and Lekakou, 2001; Ferland *et al.*, 1996; Weitzenböck *et al.*, 1999). For measurement of the in-plane permeability, two techniques are generally utilized, i.e., one-dimensional flow method and radial flow method. As fiber preforms are usually anisotropic, they have different permeability depending upon the different flow directions (Tang and Postle, 2000; Ghaddar, 1995; Pochiraju, 1999; Song *et al.*, 2002; 2004; 2005; Seong *et al.*, 2002; Cho *et al.*, 2003).

The resin flow in the thickness direction is important for thicker parts but the transverse permeability of the preform has not been investigated frequently. There are two methods for measurement of the transverse permeability: simultaneous measurement of all three principal values of the permeability tensor and independent measurement of the in-plane and the transverse permeability values. The simultaneous measurement of three principal values has been carried out in many studies (Kim and Daniel, 2003; Weitzenböck *et al.*, 1998), but it is complicated. The independent handling of the in-plane and the transverse permeability measurement is simpler than the simultaneous measurement of the principal values. In this study, we measured the transverse permeability for various preforms and compared the experimental data with numerical results.

2. Theory

2.1. Transverse permeability

Darcy's law is a commonly accepted rule for modeling fluid flow through porous media, e.g., the fibrous structure used for reinforcement.

$$\bar{u} = -\frac{\mathbf{K}}{\eta}\nabla P \tag{1}$$

where $\bar{u}$ = Darcy's velocity vector (m/s)
η = Newtonian viscosity of the fluid (Pa·s)

*Corresponding author: jaeryoun@snu.ac.kr

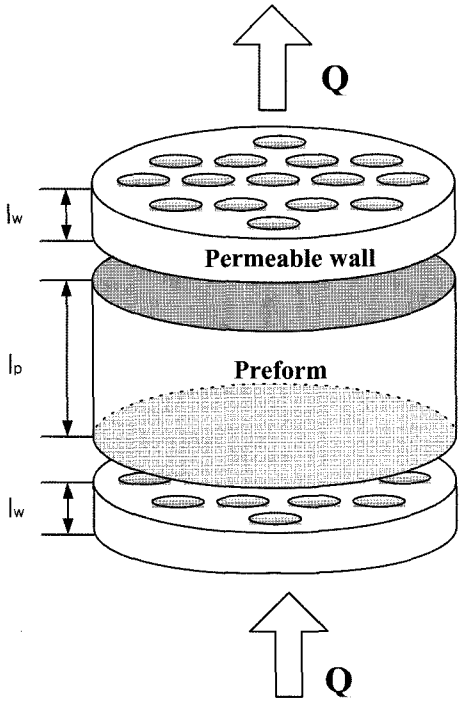

Fig. 1. Permeable wall and preform employed for measurement of the out-of-plane transverse permeability.

∇P = pressure gradient vector (Pa/m)
K = permeability tensor of the porous medium (m^2)

In this study, the out-of-plane transverse permeability is experimentally determined based on channel flow through a circular tube with cross-sectional area A and flow length *l*. The total flow length *l* is divided into flow length of the permeable solid wall, l_w, and flow length of the preform, l_p as shown in Fig. 1. Therefore, one-dimensional Darcy's law for flow through porous media can be used to calculate the transverse permeability. The one-dimensional form of Darcy's law relates the volume flow rate, *Q*, to the pressure gradient, *dP/dz*, in the direction of the flow,

$$Q = \frac{AK_z}{\eta}\frac{dP}{dz} \tag{2}$$

where K_z is a proportionality constant.

In the case of one-dimensional flow experiments, the fluid flows through the preform in one direction. After the circular tube is completely filled with fluid, steady-state data are collected by measuring the volume flow rate and the pressure drop along the flow direction. The volume flow rate *Q* is measured by weighing the fluid that has passed the flow channel.

2.2. Series model

The transverse permeability can be calculated by applying the one-dimensional Darcy's law equation. However, the transverse permeability measured by using

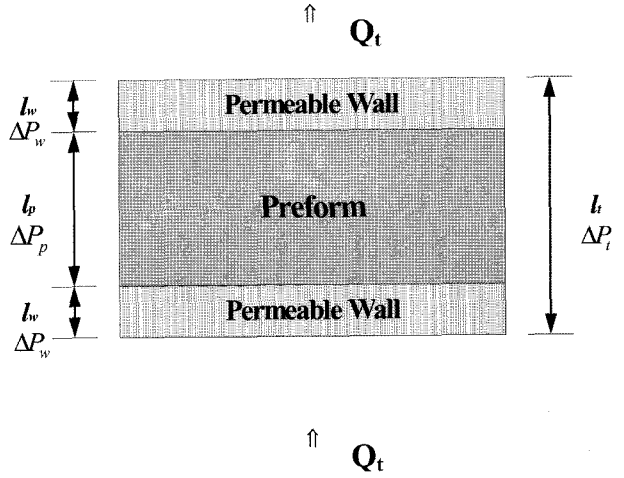

Fig. 2. Schematic diagram for series model.

the experimental set-up built in this study is affected by the transverse permeability of both permeable walls and the preform. The permeable wall was used to keep fiber volume fraction and flow length uniform. In order to obtain the transverse permeability of the preform, a series model was introduced. It was assumed that the total volume flow rate of the resin in the transverse direction of the fabric is the same as that of the permeable wall as shown in Fig. 2.

$$Q_t = \frac{A_t K_t}{\eta}\frac{\Delta P_t}{l_t} \tag{3}$$

where Q_t is the total flow rate through both the preform and the permeable wall. The total pressure drop is given as bellow.

$$\Delta P_t = \frac{Q_t \eta l_t}{A_t K_t} \tag{4}$$

The volume flow rates of the resin in the thickness direction of the preform and the permeable wall are derived as follows.

$$Q_p = \frac{A_p K_p}{\eta}\frac{\Delta P_p}{l_p} \tag{5}$$

$$Q_w = \frac{A_w K_w}{\eta}\frac{\Delta P_w}{l_w} \tag{6}$$

where

Q_t, Q_p, Q_w = total volume flow rate, volume flow rate through the preform and permeable wall

K_t, K_p, K_w = total transverse permeability, transverse permeability of the preform and permeable wall

ΔP_t, ΔP_p, ΔP_w = total pressure difference between the inlet and outlet positions, pressure difference across the preform and permeable wall

A_t, A_p, A_w = total cross-sectional area, cross-sectional area of the preform and permeable wall

l_t, l_p, l_w=total length, length of the preform and permeable wall

The pressure drop across the preform and permeable wall are expressed as follows.

$$\Delta P_p = \frac{Q_p \eta l_p}{A_p K_p} \tag{7}$$

$$\Delta P_w = \frac{Q_w \eta l_w}{A_w K_w} \tag{8}$$

The pressure drop ΔP_p acts on the preform and ΔP_w acts on the permeable wall. The total pressure drop across the entire thickness is given by adding each pressure drop.

$$\Delta P_t = \Delta P_p + 2\Delta P_w \tag{9}$$

Substitution of Eqs. (4), (7) and (8) in Eq. (9) yields

$$\frac{Q_t \eta l_t}{A_t K_t} = \frac{Q_p \eta l_p}{A_p K_p} + 2\frac{Q_w \eta l_w}{A_w K_w} \tag{10}$$

The volume flow rate is constant through each layer.

$$Q_t = Q_w = Q_p \tag{11}$$

$$\frac{l_t}{K_t}\frac{1}{A_t} = \frac{l_p}{K_p}\frac{1}{A_p} + 2\frac{l_w}{K_w}\frac{1}{A_w} \tag{12}$$

The cross-sectional area of the permeable wall (A_w), the total cross-sectional area (A_t), and the cross-sectional area of the perform (A_p) are equal. Therefore, Eq. (13) is obtained by multiplying Eq. (12) by the total area, A_t.

$$\frac{l_t}{K_t} = \frac{l_p}{K_p} + 2\frac{l_w}{K_w} \tag{13}$$

In this study, K_t, K_w, l_t, l_p, and l_w were measured by experiments. The transverse permeability of the preform can be obtained by using Eq. (13).

3. Experiments

3.1. Materials

3.1.1. Fiber preform

Five different fiber mats were used in this study. Two

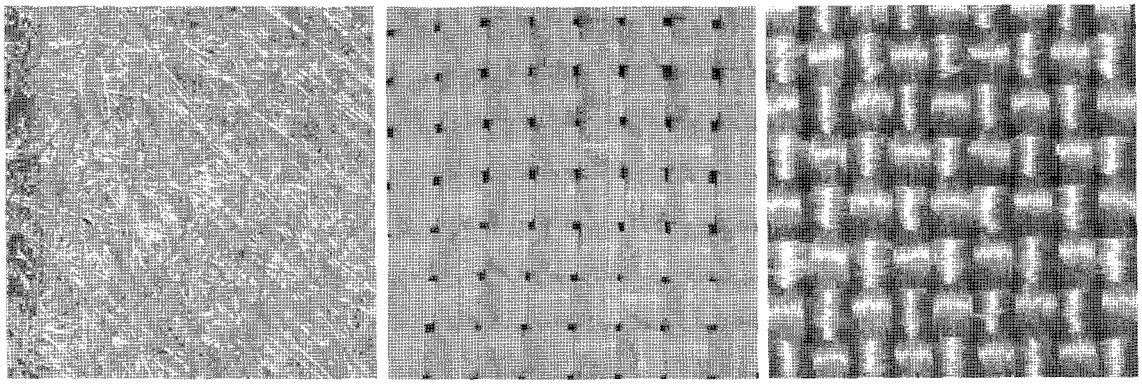

(a) Glass fiber random mat (b) Aramid fiber plain woven fabric (c) Glass fiber plain woven fabric

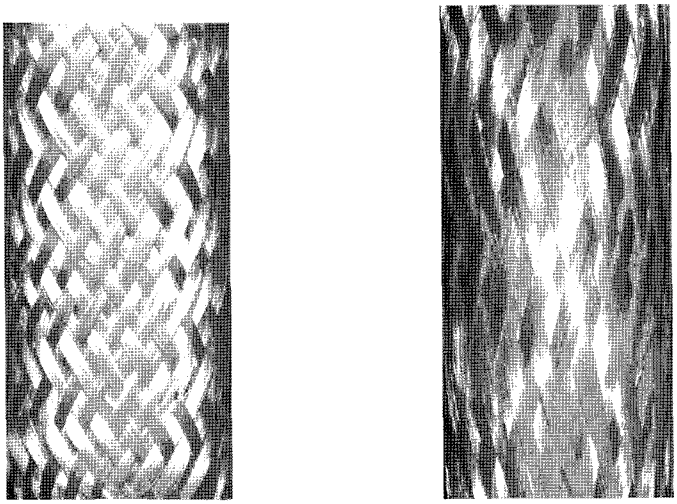

(d) Braided preform with glass fiber bundles (e) Glass-aramid fiber hybrid preform

Fig. 3. Fiber preforms used in the experiment.

fabrics were glass fiber woven fabric and aramid fiber woven fabric, and the others were glass fiber random mat, glass fiber braided preform, and glass/aramid hybrid preform (Fig. 3). The hybrid preform was used to examine the hybrid effect on the in-plane and transverse permeabilities. The braided preforms were manufactured by using a three dimensional braiding machine equipped with 48×12 carriers. The carrier of the braiding machine was activated by a pneumatic piston using compressed air and the glass fiber braided performs were produced using E-glass roving yarns. The hybrid preform was composed of aramid fiber and glass fiber bundles and had the same structure as the braided preform. The multi-axial braided preforms made by using the braiding machine have higher strength in thickness direction than the conventional multi-layer plain woven preforms.

Fiber mats were carefully placed in the cavity of the experimental mold and the orientation of fibers was preserved. In order to prevent the edge effect, the circumferential edge of the perform and the permeable wall was blocked by using a silicone grease. Since permeability is a strong function of porosity, fiber volume fraction of the preform must be determined to identify the porosity. The fiber volume fraction was varied with respect to the cavity thickness and calculated by using the following equation.

$$V_f^* = \frac{\rho_m}{\rho_f} \tag{14}$$

where V_f^* : volume fraction of fiber preform
ρ_f : density of fiber
ρ_m : density of mat

3.1.2. Resin

The test fluid used in this study was a silicone oil (dimethyl siloxane polymer, DC 200F/100CS) supplied from Dow Corning. Because the silicone oil was Newtonian fluid with the viscosity of 9.7×10^{-2} Pa·s, the Darcy's law was applied.

3.2. Experimental set-up

3.2.1. Mold design

A mold was designed and built for measurement of the transverse permeability as shown in Fig. 4. The experimental mold for measuring the permeability in the transverse direction consisted of a pair of porous circular walls and the space between them could be adjusted. Pressure was measured at the inlet and the outlet of the mold. A circular fiber mat with 12 cm diameter was cut by using a cylindrical mandrel. The parallel permeable walls with 12 cm diameter were placed in the mold. The circular preform layers were placed between the permeable walls like a sandwich. The liquid was injected in the transverse direction through the stacked fiber mats under constant inlet pressure. Four different permeable walls as shown in Fig. 5

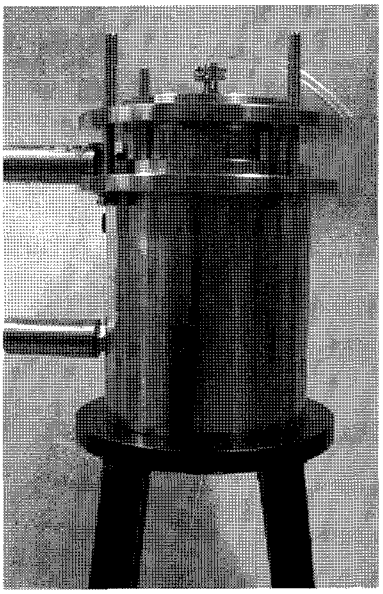

Fig. 4. Constructed mold used in the transverse flow experiment.

were tested in the experiment to investigate effects of permeable walls on the flow through the preform. The steady transverse flow was achieved by injecting the fluid through a central gate of 5 mm diameter for a sufficient period of time.

3.2.2. Experimental set-up

The Experimental set-up to characterize the transverse permeability is shown schematically in Fig. 6. Compressed nitrogen gas supplied from the supply tank was accumulated in a pressure pot. The resin was injected into the mold under constant pressure. The Pressure at the inlet and outlet position was measured with pressure transducers. It was assumed that saturation was achieved when the mass flow rate became constant and air bubbles were not observed in the silicone oil leaving the cavity. A data acquisition system collected the value of pressure at the inlet and outlet positions. The permeability was measured at different fiber volume fractions which were obtained by compressing the fiber mat to different thickness.

3.3. Measurement of the transverse permeability

The transverse permeabilities of four preforms, glass fiber random mat, glass fiber woven fabric, aramid fiber woven fabric, and glass fiber braided preform, were determined by applying a circular channel flow. To identify whether there was any difference in the permeability depending upon different permeable walls, permeability of the glass random mats with 20 layers was measured by using four different permeable walls whose permeabilities had been experimentally determined before the measurement. Different number of perform layers were placed in the cavity in order to examine the effect of compaction on the transverse permeability. The volume fraction of the pre-

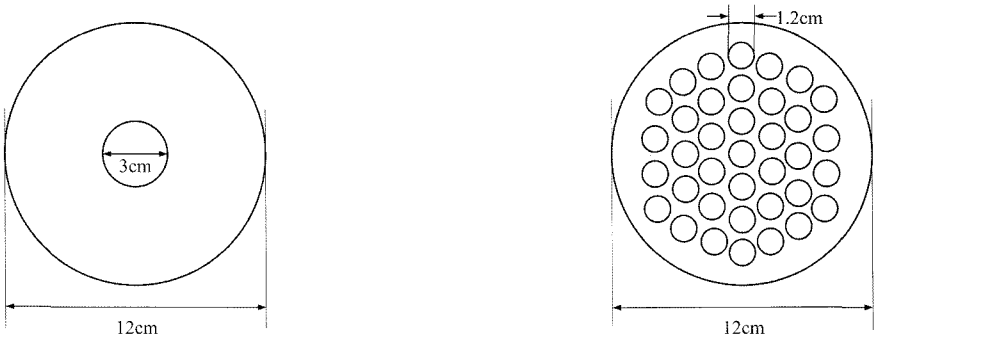

(a) Permeable wall with a circular hole (3cm diameter) in the middle

(b) Permeable wall with 37 circular holes (1.2cm diameter)

(c) Permeable wall with 85 circular holes (0.8cm diameter)

(d) Permeable wall with 68 circular holes (0.8cm diameter)

Fig. 5. Four different permeable walls used for measurement of the transverse permeability.

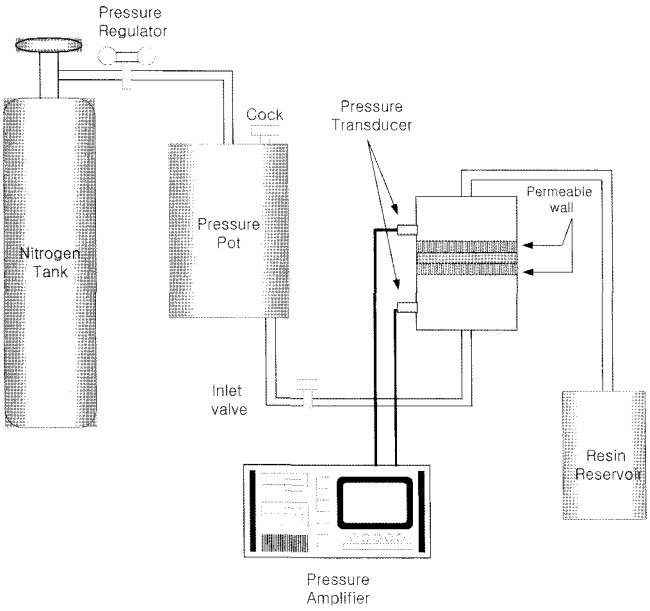

Fig. 6. Schematic diagram of the experimental setup used for measurement of the transverse permeability.

form was calculated by measuring thickness of the cavity. The flow rate at the steady state was measured by collecting the fluid exiting from the mold during measured time period and by weighing collected oil. Constant injection pressure was applied by using a pressure pot. The measurements were carried out in the saturated flow, i.e., the fibers were completely impregnated. Pressure gradient was calculated from two values of the pressure transducers. Each experiment was performed at least 5 times under the constant inlet pressure. From these data, the transverse permeability of the fiber preform was calculated through the Darcy's law.

4. Results and discussion

4.1. Influence of the permeable wall on the transverse permeability

Influence of the permeable wall on the transverse permeability was determined by using 20 layers of glass fiber random mats under constant inlet pressure. The permeability of the permeable wall was experimentally obtained without the preform between them. The transverse permeability of the fiber preform was calculated by considering the predetermined permeability of the permeable wall. The glass random mat used in the experiment has the fiber density of 2.5 g/cm^3 and the initial porosity of 0.79. Volume of the injected fluid and the exact elapsed time were measured. Two pressure values were measured by two pressure transducers located in the mold.

The permeability of each fiber preform was calculated by

Table 1. Transverse permeability of the glass fiber random mat obtained by using different permeable walls

Permeable wall	one circular hole (3 cm diameter)	37 circular holes (1.2 cm diameter)	85 circular holes (0.8 cm diameter)	68 circular holes (0.8 cm diameter)
Used fabric	Glass fiber random mat 20 layers			
Porosity	0.79			
Inlet pressure ($\times 10^5$ Pa)	0.71	0.34	0.34	0.38
Outlet pressure ($\times 10^5$ Pa)	0.13	0.21	0.21	0.20
Transverse permeability ($\times 10^{-10}$ m^2)	6.31	5.99	7.05	6.63

using the Eqs. (3), (13) and (15).

$$Q = \frac{m}{\rho_r} \tag{15}$$

where m : mass flow rate
ρ_r : density of the resin

Permeability data of the glass fiber random mat is listed in Table 1 when different permeable walls were used for the experiment. The transverse permeability was different depending upon the type of permeable walls employed. Although the transverse permeability was affected by the type of permeable walls, the difference in the permeability was not large and the average value was close to that of the permeable wall with 68 holes shown in Fig. 5(d). The selected permeable wall with 68 circular holes of 0.8 cm diameter was used for measurement of the transverse permeability.

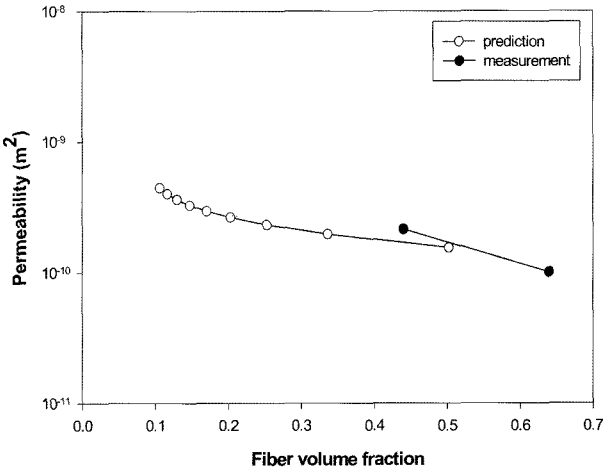

Fig. 7. Measured and predicted transverse permeability of the aramid plain woven fabric with respect to fiber volume fraction.

4.2. Comparison of numerical and experimental results for the aramid fiber woven fabric

In order to verify the experimental results, numerical analyses performed in the previous study (Song *et al.*, 2002) were utilized and compared. In the study, the in-plane and transverse permeabilities for the aramid fiber woven fabric were predicted numerically with the coupled flow model which combined microscopic and macroscopic flows. The microscopic and macroscopic flows were calculated by applying a three dimensional CVFEM (control volume finite element method) to micro and macro unit cells. Reverse and simple stacking of the aramid woven fabric was taken into account and relationship between the permeability and the preform structure such as the fiber volume fraction and stacking order was identified. Unlike other studies, the CVFEM analysis was based on more realistic three-dimensional unit cell. It was observed that the in-plane flow was more dominant than the transverse flow within the woven preform (Song *et al.*, 2002; 2004).

The aramid fiber woven fabric which had been chosen for the numerical analysis was employed for permeability measurement. The aramid plain woven fabric has the fiber density of 1.4 g/cm^3. In Fig. 7, it is shown that experimental and numerical results are in good agreement and the experimental method employed for measurement of the transverse permeability yields good results.

4.3. Comparison of the permeability obtained for glass fiber random mat, glass fiber woven fabric and aramid fiber woven fabric

Transverse permeability of the glass fiber random mat was compared with that of the glass fiber woven fabric to examine the effect of preform structure. Since low Reynolds number flows are applied to resin transfer molding, the permeability depends only on the geometry of the preform (Ghaddar, 1995). In order to determine the effect of preform structure, twenty layers of glass fiber random mats and of glass fiber woven fabrics were tested. Glass fiber random mats and glass fiber woven fabrics were considered as isotropic material in plane direction. The transverse permeability was measured at different fiber volume fractions which were achieved by compressing the fiber mat to different thickness. The transverse permeability calculated from the experimental results for each preform structure is shown in Tables 2 and 3. The transverse permeability for each glass fiber fabric was increased as the porosity was

Table 2. Transverse permeability measured with respect to porosity for 20 layers of glass fiber random mats

Porosity	0.69	0.73	0.77
Flow rate (cm^3/min)	389.00	418.38	459.09
Inlet pressure ($\times 10^5$ Pa)	0.66	0.65	0.47
Outlet pressure ($\times 10^5$ Pa)	0.18	0.17	0.19
Transverse permeability ($\times 10^{-10}$ m^2)	2.39	3.88	5.93

Table 3. Transverse permeability measured with respect to porosity for 20 layers of glass fiber woven fabrics

Porosity	0.56	0.62	0.66	0.69
Flow rate (cm^3/min)	250.36	314.02	327.41	353.48
Inlet pressure ($\times 10^5$ Pa)	0.85	0.71	0.64	0.65
Outlet pressure ($\times 10^5$ Pa)	0.11	0.14	0.17	0.17
Transverse permeability ($\times 10^{-10}$ m^2)	0.96	1.72	2.36	2.67

increased. The transverse permeability of the glass fiber random mat is lower than that of the glass fiber woven fabric at the porosity of 0.69. It can be explained by the complication of the flow path. Because the glass fiber random mat has more complex flow path than the glass fiber woven fabric, the flow through the glass fiber random mat is slower than that through the glass fiber woven fabric.

Transverse permeability of the glass fiber woven fabric and that of the aramid fiber woven fabric were measured to observe the effect of the number of perform layers. In order to observe the effect of the number of layers on the transverse permeability, two fabrics were chosen with the same structure. The experiment was carried out at the porosity of 0.59 and 0.69. The results showed the effect of the number of layers on the transverse permeability for the glass fiber woven fabric and the aramid fiber woven fabric (Figs. 8, 9 and 10). It is shown in the figures that increase in the number of perform layers reduced the permeability.

Effects of number of layers disappear when more than ten layers of the fabrics were used. It can be explained by the tortuous flow paths (Wu *et al.*, 1994) which were created due to the blocking effect at the interface between two adjacent fiber mats. However, Fig. 10 illustrates that the number of layers has higher effects in the case of aramid fiber woven fabric despite of the fact that it has the same structure as the glass fiber woven fabric. A large reduction in permeability of the aramid fiber woven fabric with respect to the number of layers can be explained by the flexibility of the aramid fiber. The aramid fiber induces higher blocking effect because the aramid fiber is more flexible and may shift more easily at the interface between the layers.

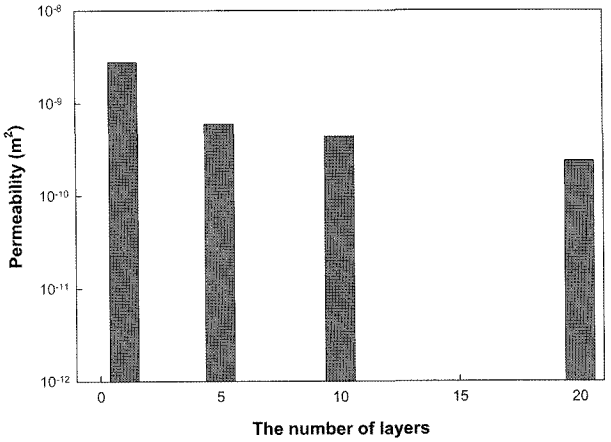

Fig. 8. Transverse permeability measured with respect to the number of layers for the glass fiber woven fabric at the porosity of 0.66.

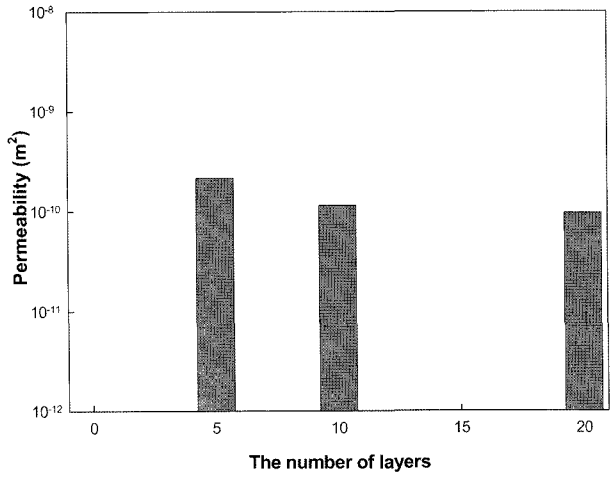

Fig. 9. Transverse permeability measured with respect to the number of layers for the glass fiber woven fabric at the porosity of 0.56.

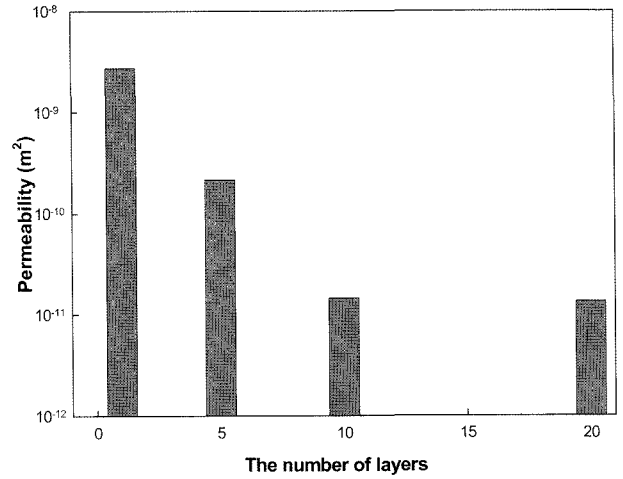

Fig. 10. Transverse permeability measured with respect to the number of layers for the aramid fiber woven fabric at the porosity of 0.56.

4.4. Transverse permeability of the braided preform

In the case of the braided preform, the transverse permeability was obtained for various porosities and number of layers. The similar procedure was repeated with the same equations to determine the transverse permeability of the braided preform. The transverse direction was set to be z-axis for the preform that was unfolded from the hollow cylindrical shape.

In order to evaluate the experimental results, numerical prediction obtained by the previous study (Song *et al.*, 2004) was compared. In the study, the complete permeability tensor for a 3-D circular braided preform was calculated by solving a boundary value problem for a periodic unit cell. The experimental results were compared with the predicted transverse permeability of the braided preform as shown in Table 4.

The transverse permeability measured for the various layers of braided preform was plotted in Figs. 11 and 12. It was found that the transverse permeability of the braided preform was increased with respect to the porosity. However, as shown in Table 4, there were some discrepancies between

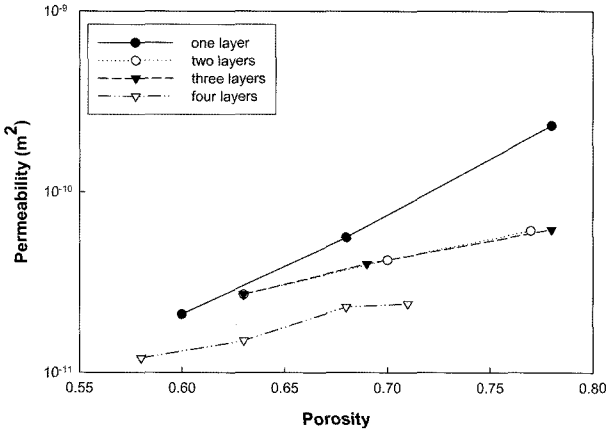

Fig. 11. Transverse permeability measured for the braided preform with respect to the porosity.

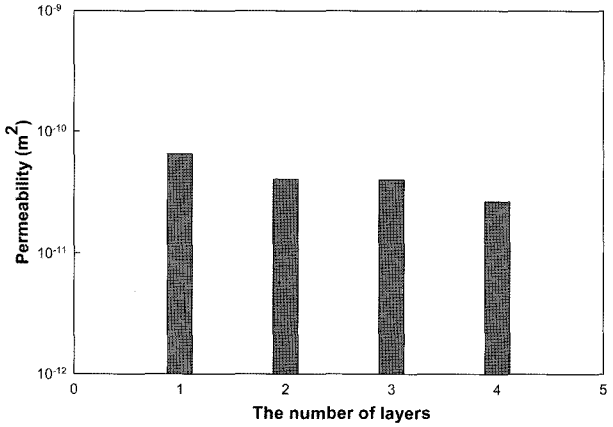

Fig. 12. Transverse permeability measured with respect to the number of layers of the braided preform at the porosity of 0.69.

Table 4. Comparison of numerical and experimental results of the braided preform

		Numerical results	Experimental results
Porosity		0.69	
In-plane permeability ($\times10^{-9}$ m^2)	x-direction	4.6	9.12
	y-direction	14.7	13.52
Transverse permeability ($\times10^{-9}$ m^2)		5.12	0.065

numerical and experimental results in the case of the transverse permeability. The differences may be attributed to the shifting and blocking of fiber tows within the layers as shown schematically in Fig. 13. A perfect unit cell is assumed for numerical calculation but the real unit cell of the braided preform may be distorted in the thickness direction during unfolding the cylindrical preform. In order to investigate the hybrid effect, in-plane permeability of the hybrid preform was measured and compared with that of the glass fiber braided preform. As shown in Table 5, there was no dif-

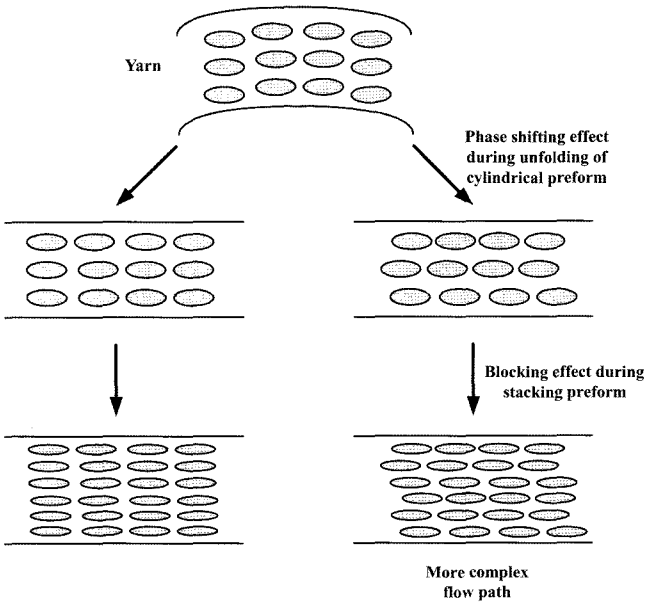

Fig. 13. Phase shifting and blocking effect during unfolding of the cylindrical braided preform.

Table 5. Comparison of the in-plane permeability for the hybrid and braided preform

		Braided preform	Hybrid preform
Porosity		0.66	
Inlet pressure ($\times10^5$ Pa)		0.35	0.42
In-plane permeability ($\times10^{-9}$ m^2)	x-direction	5.547	5.475
	y-direction	1.073	1.094

ference in the in-plane permeability between hybrid and braided preforms. It was also proven that the permeability was affected by the geometry and the porosity significantly.

5. Conclusions

Five different fiber mats were used in this study. Two fabrics were glass fiber woven fabric and aramid fiber woven fabric, and the others were glass fiber random mat, glass fiber braided preform, and hybrid braided preform. The braided preform and hybrid preform were manufactured by using a 3-D braiding machine equipped with 48× 12 carriers. Porosity and fiber volume fraction of the preform were varied by changing the cavity thickness. In order to verify the experimental data, they were compared with numerical analysis results. Experimental and numerical results of the transverse permeability were in good agreement. The transverse permeabilities of the glass fiber random mat, glass fiber woven fabric, and braided preform were measured with porosity variation. The experimental results showed that the transverse permeability was reduced as the number of layers was increased. For the braided preform, similar results were obtained. However, there are some discrepancies between numerical and experimental results in the case of transverse permeability.

Acknowledgements

This study was supported by the Korea Science and Engineering Foundation through the Applied Rheology Center (ARC). The authors are grateful for the support.

References

Advani, S. G., M. V. Bruschke and R. S. Parnas, 1994, *Flow and rheology in polymer composites manufacturing*, Elsevier, Amsterdam.

Amico, S. and C. Lekakou, 2001, An experimental study of the permeability and capillary pressure in resin-transfer moulding, *Comp. Sci. Tech.* **61**, 1945-1959.

Bechtold, G. and L. Ye, 2003, Influence of fiber distribution on the transverse flow permeability in fiber bundles, *Comp. Sci. Tech.* **63**, 2069-2079.

Cho, Y. K., Y. S. Song, T. J. Kang, K. Chung and J. R. Youn, 2003, Permeability measurement of a circular braided preform for resin transfer molding, *Fibers and Polymers* **4**, 135-144.

Drapier, S., A. Pagot, A. Vautrin and P. Henrat, 2002, Influence of the stitching density on the transverse permeability of non-crimped new concept (NC2) multiaxial reinforcements: measurements and predictions, *Comp. Sci. Tech.* **62**, 1979-1991.

Endruweit, A., T. Luthy and P. Ermanni, 2002, Investigation of the influence of textile compression on the out-of-plane permeability of a bidirectional glass fiber fabric, *Polym. Compos.* **23**, 538-554.

Ferland, P., D. Guittard and F. Trochu, 1996, Concurrent Methods for Permeability Measurement in Resin Transfer Molding, *Polym. Compos.* **17**, 149-158.

Gebart, R. R. and P. Lidström, 1996, Measurement of in-plane permeability of anisotropic fiber reinforcements, *Polym. Compos.* **17**, 43-51.

Ghaddar, C. K., 1995, On the permeability of unidirectional fibrous media: a parallel computational approach, *Phys. Fluids.* **11**, 2563-2586.

Jones, R.M., 1975, *Mechanics of composite materials*, Scripta Book Company, Washington.

Kim, S. K. and I. M. Daniel, 2003, Determination of three-dimensional permeability of fiber preforms by the inverse parameter estimation technique, *Composites Part A* **34**, 421-429.

Lim, S. T. and W. I. Lee, 2000, An analysis of the three-dimensional resin-transfer mold filling process, *Comp. Sci. Tech.* **60**, 961-975.

Markicevic, B. and T. D. Papathanasiou, 2003, A model for the transverse permeability of bi-material layered fibrous performs, *Polym. Compos.* **24**, 68-82.

Phelan Jr, F. R. and G. Wise, 1996, Analysis of transverse flow in aligned fibrous porous media, *Composites Part A* **27**, 25-34.

Pochiraju, K., 1999, Three-dimensionally woven and braided composites. : An experimental characterization, *Polym. Compos.* **20**, 733-747.

Sadiq, T. A. K., S. G. Advani and R. S. Parnas, 1995, Experimental investigation of transverse flow through aligned cylinders, *Int. J. Multiphase Flow* **21**, 755-774.

Sayre, J. R. and A. C. Loos, 2003, Resin infusion of triaxially braided preforms with through-the-thickness reinforcement, *Polym. Compos.* **24**, 229-236.

Seong, D. G., K. Chung, T. J. Kang and J. R. Youn, 2002, A study on resin flow through a multi-layered preform in resin transfer molding, *Polym. Polym. Compos.* **10**, 492-519.

Song, Y. S., K. Chung, T. J. Kang and J. R. Youn, 2002, Prediction of permeability tensor for plain woven fabric by using control volume finite element method, *Polym. Polym. Compos.* **11**, 465-476.

Song, Y. S., K. Chung, T. J. Kang and J. R. Youn, 2004, Prediction of permeability tensor for three dimensional circular braided preform by applying a finite volume method to a unit cell, *Comp. Sci. Tech.* **64**, 1629-1636.

Song, Y. S., K. Chung, T. J. Kang and J. R. Youn, 2005, Numerical Prediction of Permeability Tensor for Three Dimensional Circular Braided Preform by Considering Intra-tow Flows, *Polym. Polym. Compos.* **13**, 323-334.

Tang, Z. X. and R. Postle, 2000, Mechanics of three-dimensional braided structures for composite materials-Part I: fabric structure and fiber volume fraction, *Compos. Struct.* **49**, 451-459.

Weitzenböck, J. R., R. A. Shenoi and P. A. Wilson, 1998, Measurement of three-dimensional permeability, *Composites Part A* **29**, 159-169.

Weitzenböck, J. R., R. A. Shenoi and P. A. Wilson, 1999, Radial flow permeability measurement. part B: application, *Composites Part A* **30**, 797-813.

Wu, C. H., T. J. Wang and L. J. Lee, 1994, Trans-plane fluid permeability measurement and its applications in liquid composite molding, *Polym. Compos.* **15**, 289-298.